Contents lists available at ScienceDirect

Remote Sensing of Environment

journal homepage: www.elsevier.com/locate/rse

Capturing tree crown formation through implicit surface reconstruction using airborne lidar data

Akira Kato [a,*], L. Monika Moskal [b], Peter Schiess [b], Mark E. Swanson [c], Donna Calhoun [d], Werner Stuetzle [e]

[a] *Graduate School of Horticulture, Chiba University, 648 Matsudo, Matsudo-shi, Chiba 271-8510, Japan*
[b] *Precision Forestry Cooperative, College of Forest Resources, University of Washington, Box 352100, Seattle, WA 98195-2100, USA*
[c] *Department of Natural Resource Sciences, Washington State University, Pullman, WA 99164-6410, USA*
[d] *DM2S/SFME/LTMF Bt 454, Commissariat a l'Energie Atomique, Centre de Saclay, 91191 Gif-sur-Yvette, France*
[e] *Department of Statistics, College of Arts and Sciences, University of Washington, Box 353765, Seattle, WA 98195-3765, USA*

ARTICLE INFO

ABSTRACT

Forest structure data derived from lidar is being used in forest science and management for inventory analysis, biomass estimation, and wildlife habitat analysis. Regression analysis dominated previous approaches to the derivation of tree stem and crown parameters from lidar. The regression model for tree parameters is locally applied based on vertical lidar point density, the tree species involved, and stand structure in the specific research area. The results of this approach, therefore, are location-specific, limiting its applicability to other areas. For a more widely applicable approach to derive tree parameters, we developed an innovative method called 'wrapped surface reconstruction' that employs radial basis functions and an isosurface. Utilizing computer graphics, we capture the exact shape of an irregular tree crown of various tree species based on the lidar point cloud and visualize their exact crown formation in three-dimensional space. To validate the tree parameters given by our wrapped surface approach, survey-grade equipment (a total station) was used to measure the crown shape. Four vantage points were established for each of 55 trees to capture whole-tree crown profiles georeferenced with post-processed differential GPS points. The observed tree profiles were linearly interpolated to estimate crown volume. These fieldwork-generated profiles were compared with the wrapped surface to assess goodness of fit. For coniferous trees, the following tree crown parameters derived by the wrapped surface method were highly correlated ($p<0.05$) with the total station-derived measurements: tree height ($R^2=0.95$), crown width ($R^2=0.80$), live crown base ($R^2=0.92$), height of the lowest branch ($R^2=0.72$), and crown volume ($R^2=0.84$). For deciduous trees, wrapped surface-derived parameters of tree height ($R^2=0.96$), crown width ($R^2=0.75$), live crown base ($R^2=0.53$), height of the lowest branch ($R^2=0.51$), and crown volume ($R^2=0.89$) were correlated with the total station-derived measurements. The wrapped surface technique is less susceptible to errors in estimation of tree parameters because of exact interpolation using the radial basis functions. The effect of diminished energy return causes the low correlation for lowest branches in deciduous trees ($R^2=0.51$), even though leaf-off lidar data was used. The wrapped surface provides fast and automated detection of micro-scale tree parameters for specific applications in areas such as tree physiology, fire modeling, and forest inventory.

© 2009 Elsevier Inc. All rights reserved.

1. Introduction

The accurate measurement of tree crown parameters is critical for fields such as wildland fire dynamics (Agee, 1993; Finney, 1998), plant physiology (Maguire & Hann, 1989; Oohata & Shinozaki, 1979; Shinozaki et al., 1964) forest health monitoring (Zarnoch et al., 2004; Schomaker et al., 2007), and habitat analysis (Lowman & Rinker, 2004). The shape and size of tree crowns are typically related to photosynthesis, nutrient cycling, energy transfer (evapotranspira-

tion and respiration) and light transmittance to understory vegetation. Obtaining precise crown information is, however, a challenging task, because the irregularity of many crown shapes is difficult to capture using standard forestry field equipment. Tree crown shapes have attracted the interests of artists as well. Christo and Jeanne-Claude used fine fabric to wrap actual trees and emphasize the complexity of the crown shape (Fig. 1). Their artistic approach to visualize the complexities of tree crowns prompted us to attempt the same but relying on mathematical and computer graphic techniques applied to light detection and ranging (lidar) point clouds.

Lidar systems have been used for ecological applications, change detection studies, forest inventory applications, and single-tree based methods (Carson et al., 2004). There are two kinds of lidar systems that have been used in previous research: discrete-return devices (DRD) and full wave recording devices (WRD) (Lefsky et al., 2002;

* Corresponding author.
   E-mail addresses: akiran@faculty.chiba-u.jp (A. Kato), lmmoskal@u.washington.edu (L.M. Moskal), schiess@u.washington.edu (P. Schiess), markswanson@wsu.edu (M.E. Swanson), donna.calhoun@cea.fr (D. Calhoun), wxs@u.washington.edu (W. Stuetzle).

Fig. 1. Visualization of tree crown formation captured by the artwork of Christo and Jean-Claude. (Christo and Jeanne-Claude, Wrapped Trees, Fondation Beyeler and Berower Park, Riehen, Switzerland 1997–98, Photo: Wolfgang Volz, ©Christo 1998).

Patenaude et al., 2004). WRD research focuses primarily on plot-level estimation of canopy structures because of the larger footprint size. The process of validation with field-measured tree parameters relies on summarizing field data at the plot level and varies with user interpretation (Mean et al., 1999). Since DRD captures returns from individual structures, it can provide more direct measurement of individual tree crown parameters. Most DRD data, however, has been analyzed with regression analysis of canopy quantile lidar metrics (Lim & Treitz, 2004; Næsset & Økrand, 2002) or the fitting of an assumed geometric shapes to derive crown parameters such as height or crown width (Andersen et al., 2002; Persson et al., 2002; Riaño et al., 2004). These approaches had two main drawbacks. First, information specific to the tree species related to their unique crown shape was required to quantify crown parameters from lidar-derived metrics. Species identification from remotely sensed data is still under development. Thus, a species-invariant approach should be considered for lidar applications. Second, regression models for fitting crown shapes were derived and applied on a local basis. The modeled regression cannot be applied to the other areas without risking errors of extrapolation. Thus, a widely applicable, individual tree-specific approach to derive tree parameters is highly advantageous for further automated detection of crown geometry from lidar measurement.

A number of commonly employed tree parameters are tree height, crown width, basal area, crown base height, and crown volume. Previous research on the determination and utilization of these parameters from DRD data is reviewed in the following paragraphs of this paper according to each tree parameter, because sensor settings and data characteristics differ between DRD and WRD.

Lidar-derived tree height information has been used for tree growth estimation and stem location (Hopkinson, 2007; Yu et al., 2004), detection of single or multi-story stand condition (Zimble et al., 2003), estimation of carbon density (Patenaude et al., 2004), biomass estimation (Bortolot & Wynne, 2005), and modeling the distribution of understory vegetation (Gobakken & Næsset, 2004, 2005; Maltamo et al., 2004). Generally, tree height and stem location are derived from a Digital Canopy Height Model (DCHM) which is the elevation difference between Digital Surface Models (DSMs) and Digital Terrain Models (DTMs). Convex shapes of the DCHM were assumed to be crown structure and were used to detect tree tops. The location and height of the tree tops were key factors for determining stem location and stand density (Hyyppä et al., 2001). The measurement of tree height depends on the quality of Digital Terrain Models

(DTMs) (Andersen et al., 2006; Yu et al., 2004). Since tree height is generally a more accurately determined parameter than other crown or canopy parameters, tree height is preferred to detect change in tree growth studies.

Crown width and basal area have been derived from lidar data with the use of regression models (Means et al., 2000) or the segmentation method (Morsdorf et al., 2004; Persson et al., 2002; Popescu & Zhao, 2007). Means et al. (2000) used stepwise regression analysis for 50 m×50 m field plot to get R^2 of 0.95 (R^2: correlation coefficient) for basal area between field and lidar measurement. For individual trees, Persson et al. (2002) used the active contour technique to retrieve crown diameter from lidar-derived DCHM to achieve an R^2 of 0.76, while Popescu and Zhao (2007) used a voxel-based method to get R^2 of 0.51.

Crown base height has been estimated with stepwise regression models (Næsset & Økrand, 2002) to achieve R^2 of 0.53 for individual trees. Alternatively, a median filter was applied to the vertical lidar point distribution (Holmgren & Persson, 2004) to get an R^2 of 0.71, while a voxel-based method (Popescu & Zhao, 2007) yielded R^2 values between 0.73 and 0.78. The accuracy of crown width and live crown base measurements relies on the precise segmentation of points for individual trees, both horizontally and vertically.

Crown volume, one of the most difficult tree parameters to obtain, is required for avian habitat analysis (Hinsley et al., 2002), estimation of the fractal dimension of trees (Zeide & Pfeifer, 1991), and forest fire simulation (Finney, 1998). Crown volume has been estimated using fitted explicit geometric equations (e.g., cones and ellipsoids) using diameter at breast height (DBH), field-measured basal area, crown diameter, and tree height as the independent variables. It also requires characterization of crown curvature (Nelson, 1997; Sheng et al., 2001). Riaño et al. (2004) computed crown volume using a relative crown height profile given by vertical lidar point density and distribution. None of these modeled equations are capable of exact fitting to all types of tree shapes, even within the same species.

To estimate those tree parameters, tree canopy shapes have been reconstructed by three different ways: implicitly, explicitly, and parametrically. The parametric reconstruction has been approached by regression statistical analysis, and the explicit reconstruction has been done using mathematical explicit functions such as cone, ellipsoid, parabolic and a combination of those. The implicit reconstruction has been accomplished with a "marching cubes" method with the implicit function (Angel, 2003).

Other approaches to quantify the crown shapes using a parametric approach are stochastic modeling and the crown shell modeling. Biging and Gill (1997) used time series analysis to predict the vertical crown profile and Song et al. (1997) used a crown shell model to generate a 3D tree crown model for ecological simulation. These approaches used limited sampled information of crown profiles. But lidar can provide much richer point data for detailed reconstruction of crown architecture.

With more lidar point returns, an accurate and direct way to capture the object from lidar returns should be considered. Thomas et al. (2006) used datasets with two different lidar point densities on the effectiveness of the regression approach. Lower point density lidar estimates were better for tree height and basal area while higher point density was better suited to capture crown closure (Thomas et al., 2006). Although the local variability is better captured by high point density (20 points m^{-2} is used for our research), it cannot be adequately analyzed using regression analysis to get all tree parameters. An alternative approach should be taken for higher density lidar, which is becoming more widely available. Furthermore, building regression models for different species and tree shapes requires costly sampling to characterize the general tree shape for each species in the research area. Managed forests are well described with regression models based on a few sample plots given the relative uniformity. Urban forests with their mix of species and high variability in shapes cannot be described very well with regression models.

An alternative approach is a voxel-based reconstruction (Lefsky et al., 1999; Phattaralerphong & Sinoquet, 2005; Popescu & Zhao, 2007). Lefsky et al. (1999) used a canopy volume method to quantify the region of vertical distribution of WRD data. Popescu and Zhao
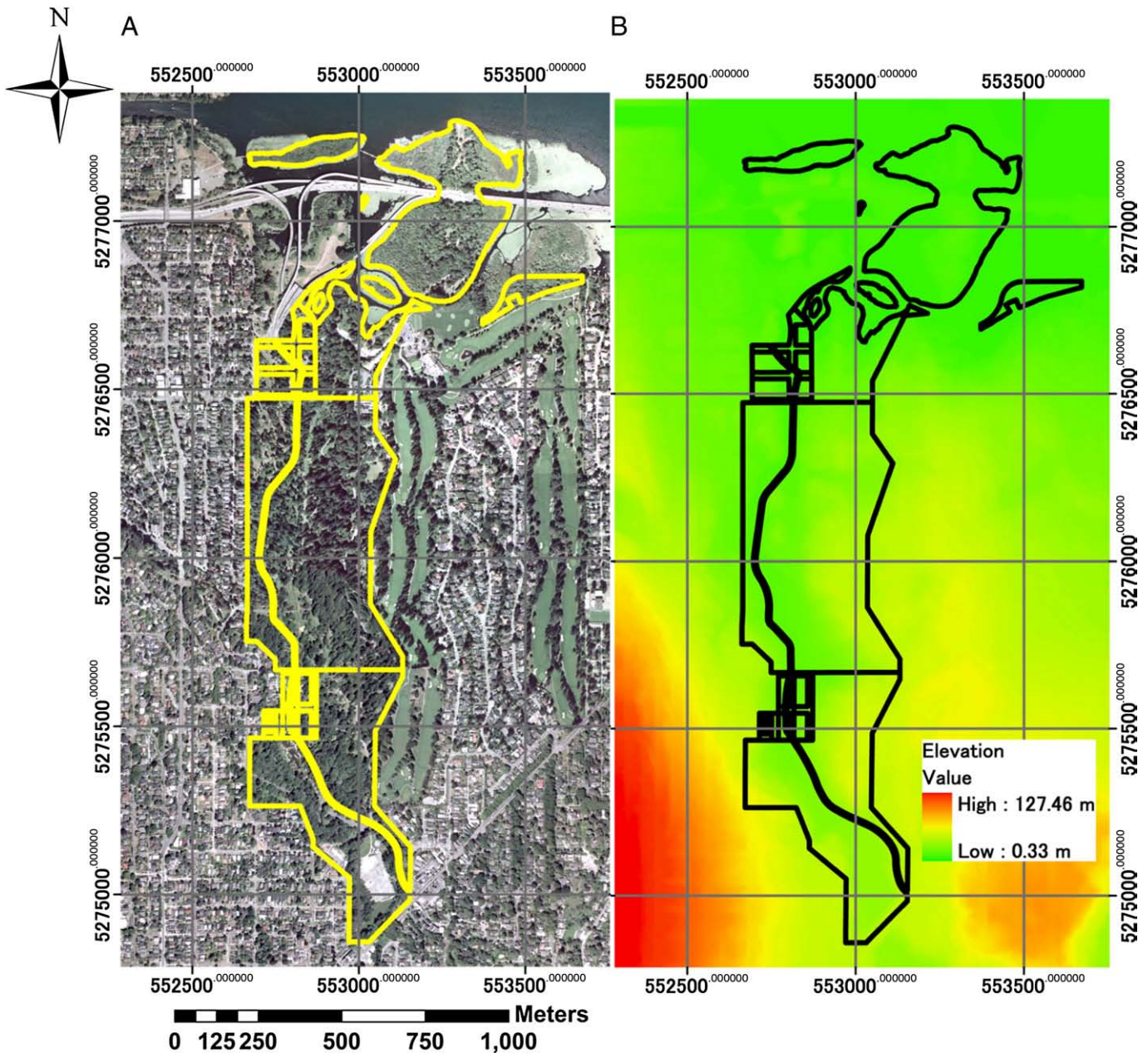

Fig. 2. Our research site is in Washington Park Arboretum, Seattle WA. The yellow boundary on the left and black boundary on the right displays the research site. A true-color digital orthophoto (1:12,000 sale, A) and DEM (30 m × 30 m, B) come from USGS the National Map Seamless Server. Right image (B) is a color representation of the DEM, showing the generally moderate relief of the study site. (For interpretation of the references to color in this figure legend, the reader is referred to the web version of this article.)

(2007) used a voxel approach for DRD data. Phattaralerphong and Sinoquet (2005) used a photo interpretation technique and ray-box intersection to reconstruct voxels for a crown shape. A drawback to this voxel-based method for DRD was the fact that the total crown volume was calculated by the sum of the voxels. The volume, therefore, depended on the spatial allocation and voxel resolution. The generation of voxels in three-dimensional spaces was influenced by the degree of laser penetration through the canopy. Voxel-based approaches work better for WRD than DRD because of the tendency of WRD sensors to capture the lower strata of the canopy. DRD returns, however, tend to reflect from the surface of the canopy (Lefsky et al., 1999). To get more exact shape of canopy formation from lidar points, implicit interpolation is employed to reconstruct the tree shape in this study to avoid the spatial holes among voxels and to obtain a more exact shape of complex tree crowns.

Implicit surface reconstruction has been widely used in the field of computer graphics to construct 3D models of physical objects from noisy scanned laser points (Bloomenthal et al., 1997). Radial basis functions (RBFs) were used, as were implicit functions of an isosurface (Bishop, 2005; Carr et al., 1997, 2001, 2003; Wendland, 2005), and were used for classification to find the shortest path in a neural network (Bishop, 2005). There have been several ways to reconstruct surfaces from laser ranging data. In general, the subdivision surface approach (Bloomenthal et al., 1997) and the Non-Uniform Rational B-Spline (NURB) surface (Shirley, 2005) were utilized. The common characteristics of these methods were that they did not perform an exact interpolation and did require a complex procedure to reconstruct the shape. The RBF approach is, however, an exact interpolation method means that interpolated vectors pass exactly through all input points. The wrapped surface interpolated by RBFs in this study fits the input lidar point location.

To validate the results of the surface reconstruction, a new field validation technique for crown analysis was developed. The technique of field-measured crown geometry has not been addressed by previous research and it requires accurate horizontal and vertical angular measurement. Handheld devices are commonly used to measure these angles efficiently over a large area. Lidar, however, generates much more accurate three-dimensional coordinates than a handheld device can. Human manual error, therefore, should be minimized to validate lidar-derived tree parameters. In this study, a survey total station (Nikon-Trimble Inc., USA) was utilized to validate lidar-derived tree parameters and crown profiles. Moreover, we computed field-measured crown volume from crown profiles (the edges of tree crown shapes) from four different cardinal angles. The field based crown volume is compared with the volume given graphically by the wrapped surface.

2. Objectives

We introduce a species-invariant method for deriving tree parameters from lidar discrete points using implicit surface reconstruction (a wrapped surface reconstruction). In this research, we apply this approach to a mixed species urban forest. Our research aims to: 1) analyze the relationship of tree parameters derived from the wrapped surface and field measured crown parameters (tree height, crown width, live crown base, height of the lowest branch, and crown volume, and 2) quantify the error associated with the wrapped surface.

3. Study area

The research area is located in the Washington Park Arboretum at the south end of the University of Washington and east of downtown Seattle, WA (Fig. 2). The total area is 230 acres. The arboretum collection contains 5500 different species ranging from shrubs to trees. The terrain of our study area is moderate in slope, and the site is in a relatively urban

Table 1
Species list for sampled coniferous trees.

	Coniferous (26)	Summary	
Abies (1)	Grand fir, *A. grandis* (1)	Sample size (# trees)	26
Cedrus (2)	Atlas cedar, *C. atlantica* (1)	Tree height (m)	9.2–39.9
	Cedar of Lebanon, *C. libani* (1)	Crown base height (m)	0–26.1
Picea (2)	Norway spruce, *P. abies* (1)	Crown diameter (m)	2.8–11.2
	Sakhalin spruce, *P. glehnii* (1)	Crown volume (m^3)	77.4–3189.3
Pinus (5)	Eastern white pine, *P. strobes* (1)	DBH (cm)	25.5–117
	Knobcone pine, *P. attenuate* (1)	Lowest live branch (m)	0–25.4
	Maritime pine, *P. pinaster* (2)		
	Montezuma pine, *P. montezumae* (1)		
Pseudotsuga (6)	Douglas-fir, *P. menziesii* (6)		
Thuja (9)	Western red cedar, *T. plicata* (9)		
Tsuga (1)	Mountain hemlock, *T. mertensiana* (1)		

setting. Stands are heterogeneous, multi-aged mixtures of tree species from around the temperate world. It is an ideal setting in which to test a methodology for characterizing irregular tree crowns and for the development of methods that characterize tree structure without destructive or excessive sampling in the field.

4. Field data

Even though the accuracy of airborne lidar and the detail of objects measured by the data have improved, field validation of the tree crowns derived from lidar data has not been well developed. The tools used to verify airborne lidar-derived parameters must have a similar level of precision as the lidar data itself. A ground-based lidar can be used for this purpose. However, the methodology to use the ground-based lidar for this aim is still in a stage of development. Issues such as underestimation of tree parameters (Chasmer et al., 2006), inability to distinguish between laser returns from foliage and stems (Clawges et al., 2007), and misalignment of points captured by different vantage points (Henning & Radtke, 2006) continue to challenge verification methods that employ ground lidar. Furthermore, the point density captured by the ground-based lidar is much higher than the density of point samples necessary to characterize the crown formation. The total station was, therefore, used for verification of this research.

We used subjective random sampling to collect data for 55 open canopy and overstory trees (26 coniferous trees and 29 deciduous trees) to obtain the crown profiles using the total station for field validation. Vertically overlapping ('overtopped') trees were excluded from this analysis. The species and the statistics of field measured tree parameters are given in Table 1 (coniferous) and Table 2 (deciduous). The field-measured tree parameters captured by the total station (Nikon DTM-420) are summarized on the right of both tables.

The total station is a high-end surveying device and has been found to be highly efficient equipment for forest measurement purposes (Kiser et al., 2005). Kiser et al. (2005) calculated the efficiency of various types of field equipment and rated them on the basis of field worker cost and closing accuracy, concluding that the total station was the best instrument for fieldwork among those surveyed. The field measurement methodology in this study is demonstrated in Fig. 3. To capture crown profiles, vertical and horizontal angles to either side of the tree were measured from four positions around the tree. These positions were separated by 45° azimuth angles around the stem location, and were located at a horizontal distance from the tree of at least 4–5 times the width of the crown. This ensures that tangential angles to the edge of the tree crown represent the actual profile silhouette of the measured tree. The distance range of this observation was set relative to tree size, because the precision of angular measurement using the total station decreases as the distance

Table 2
Species list for sampled deciduous trees.

	Deciduous (29)	Summary of tree parameters	
Acer (5)	Sugar maple, *A. saccharum* (1)	Sample size (# trees)	29
	Maple *A. sp.* (4)	Tree height (m)	13.4–39.3
Alnus (2)	Italian alder, *A. cordata* (1)	Crown base height (m)	0–5.2
	Red alder, *A. rubra* (1)	Crown diameter (m)	3.8–15.8
Betula (1)	Birch, *B. sp.* (1)	Crown volume (m³)	305.4–5627
Carya (2)	Hickory, *C. sp.* (2)	DBH (cm)	20.5–111.5
Castanea (2)	Japanese chestnut, *C. crenata* (2)	Lowest live branch (m)	0–6.5
Catalpa (2)	Hybrid catalpa, *C. erubescens* (2)		
Crataegus (3)	Black hawthorn, *C. douglasii* (1)		
	Hawthorn, *C. sp.* (2)		
Fraxinus (2)	Oregon ash, *F. latifolia* (2)		
Liriodendron (1)	Tulip tree, *L. tulipifera* (1)		
Paulownia (1)	Empress tree, *P. tomentosa* (1)		
Populus (2)	Popular, *P. sp.* (2)		
Quercus (4)	Northern red oak, *Q. rubra* (1)		
	English oak, *Q. rubur* (1)		
	Oak, *Q. sp.* (2)		
Tilia (2)	Caucasus linden, *T. caucasica* (1)		
	Japanese lime tree, *T. japonica* (1)		

between the tree stem and the instrument increases. The vertical angles that can be measured by the total station have an upper limit of about 55°, which means that the total station must be located a certain minimum distance from the tree. From each vantage point, the horizontal angle to the crown edge was recorded vertically every fixed 5° increments, beginning from the closest 5° vertical angle interval of the lowest lateral branches. Essentially, the visual silhouette of the tree was captured in coordinate space. In addition to these points, the locations of treetop and trunk base height were recorded. Crown base height was defined as the height of the lowest live branch on stem. The height of the lowest branch was also collected for each profile. From one vantage point, two crown

profiles were taken and each crown profile was created by linearly interpolated lines. Each observation point could capture two crown profiles. Four observation points, therefore, covered eight crown profiles. To get the crown volume of a tree, the vertical profile was integrated every 45° for each profiling direction. The sum of them was the total volume for a tree from field observation. To get a more precise volume, the volume enclosed between live crown base and height of the lowest side branch was subtracted from the total volume. Diameter at breast height was also measured. The reflector target was not used for crown edge measurement, but only to measure the horizontal distance from the total station to the stem. The location of all crown edge points was calculated trigonometrically from the vertical and horizontal angle based on the horizontal distance (HD) between the instrument and the stem.

The location of the total station required a relatively clear view of the entire crown from four sub-cardinal angles. Field measurements for coniferous trees were, therefore, conducted during the deciduous leaf-off season to get a clear view from the instrument. The field measurement season for deciduous trees was conducted during the growing season to get a clear view of tree crown edges. The field season was between February and March 2007 for coniferous trees and between May and August 2007 for deciduous trees.

All vantage points were georeferenced with GPS (Global Positioning System) location collected with survey-grade Trimble Pathfinder Pro XR GPS units (Nikon-Trimble Inc., USA). All GPS points were differentially corrected with correction data from one of the closest NOAA CORS (National Oceanic and Atmospheric Administration Continuously Operating Reference Stations).

5. Lidar data

A small-footprint airborne lidar dataset was acquired over this research site in 2005. The lidar sensor characteristics are shown in Table 3. The coordinate system of data associated with this lidar system is NAD83 UTM 10N. The flight campaign was conducted during leaf-off season with average altitude 900 m and 20° scan angle. There is a two-year difference between the lidar acquisition (March, 2005)
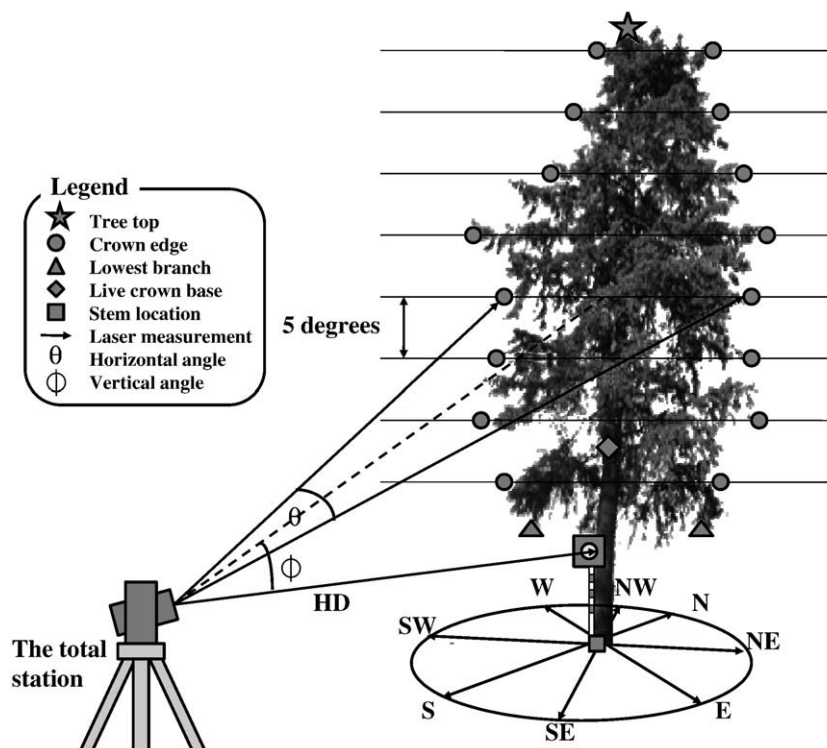

Fig. 3. Field method of crown formation captured by the total station.

Table 3
Airborne lidar sensor system.

Date of acquisition	March 17th, 2005 (leaf-off)
Platform	Airborne
Scan angle	20° (10° from Nadir)
Laser sensor	Optech ALTM 3100
Flying height	900 m
Impulse frequency	100 kHz
Laser point density range	Average for dataset: 3 to 20 points m^{-2}
	Average for study trees: 10–20 points m^{-2}

and the field measurements (from Jan. to May, 2007). To capture the detail of tree crown structure, we tested our method using higher point density than previous studies. The point density was greater than 9 points m^{-2} for each flight line. The point sampling is related to the degree of the overlap of measurement swaths. The point density (diverges from 10 to 20 points m^{-2}) is, therefore, not homogenous over this research site and the average point density of sampled trees used in this study was 10 to 20 points m^{-2}. The effect of point density for this method must be addressed by future studies.

6. Methodology

The steps involved in our crown wrapping approach are shown in Fig. 4. The sequence of operations is composed of three sections: pre-processing, post-processing, and field validation. Each section has several sub-sections.

6.1. Pre-processing

Pre-processing includes the creation of a Digital Canopy Height Model (DCHM) from the difference between DTMs and DSMs. To create DTMs, a new algorithm was used to classify the lidar points for the canopy and ground returns. Local minimum height surfaces and RBFs interpolation were used to create DTMs. Smith et al. (2005) tested one geostatistical method (ordinary kriging) and four local deterministic methods (bilinear, bicubic, nearest neighbor, and biharmonic spline interpolations) with airborne laser data in creating DSMs of urban areas. On one hand, these deterministic methods required regularly spaced points and introduced errors because of their smoothing algorithms. On the other hand, the geostatistical method is used for irregularly scattered points but is not an exact interpolator. RBFs involve the exact interpolation and, therefore, are effective for irregularly scattered points.

Local minimum height lidar points were collected within 1 m × 1 m square grids to make the minimum height elevation models. The minimum height model, however, contains some returns from the top of the crown and sometimes a few returns from the trunk or lower branches. Since our study area had moderate slope, within 20 m × 20 m extracted area around our sampled trees the mean and one standard deviation of the elevation values were applied to filter out non-ground returns. With the filtered ground points, the initial DTMs were created using RBFs. The initial DTMs were used to pick more ground points from original lidar returns. Then RBFs were applied again for the selected points to create the final DTMs. Fig. 5 shows the selected lidar points and the final DTMs using RBFs.
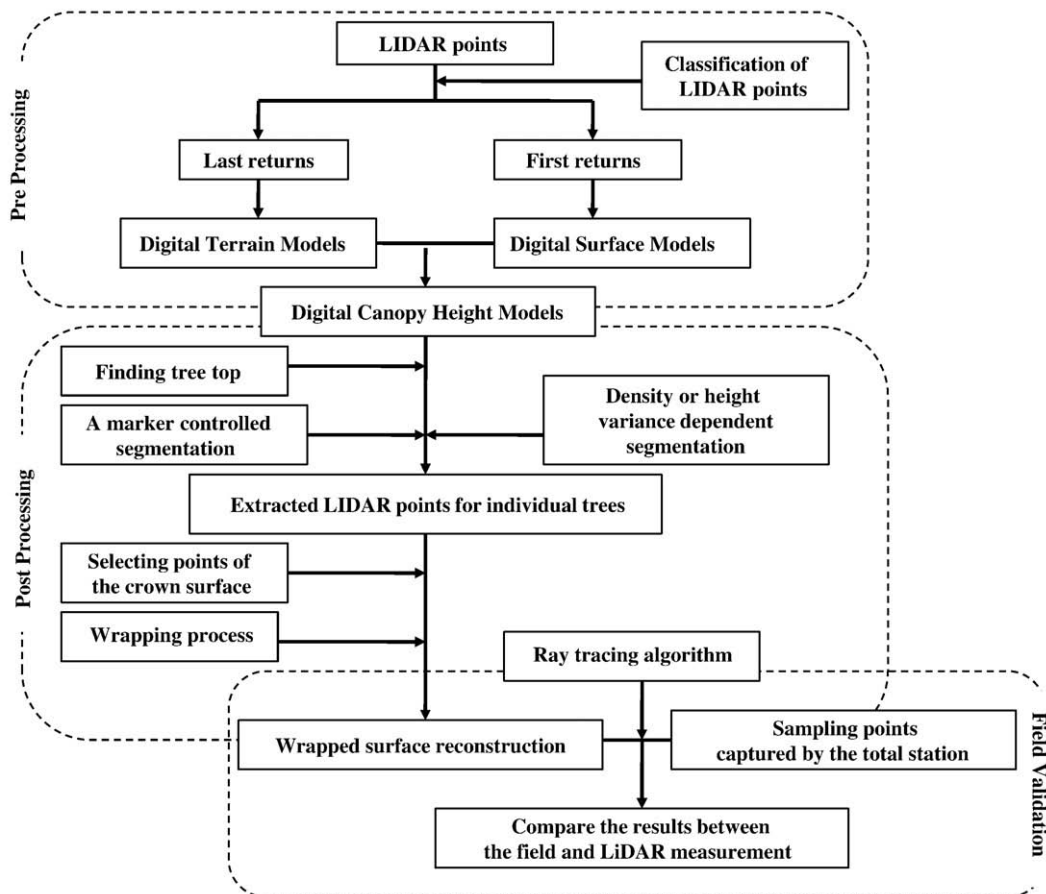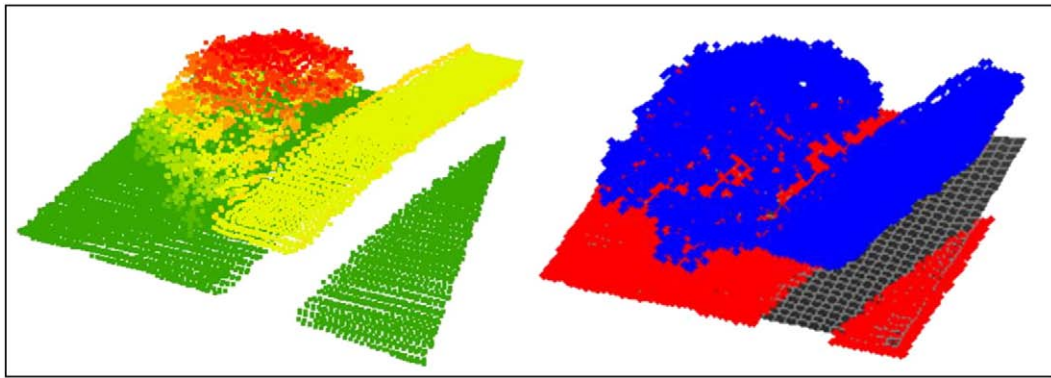
Fig. 4. Overview of methodology.

Fig. 5. DTMs created by RBFs. In the image at left, all lidar point distribution are colored by height. Yellow stripe points represent an elevated highway adjacent to the tree blocking the ground surface underneath. In the image at right, the DTM is shown in gray, classified ground returns by red, and classified canopy returns by blue. DTM was successfully created underneath the highway as well. (For interpretation of the references to color in this figure legend, the reader is referred to the web version of this article.)

Pouderoux and Gonzato (2004) also used RBFs to reconstruct DTMs in a large area of Mt. Washington and Mount St. Helens with edge points sampled from contour lines created from USGS DEM. They used a hierarchical data structure to partition the data to reconstruct the surface locally and combined all local surfaces to generate single DTM layer. For computational efficiency, instead of making a single DTM layer of the entire research area ground returns of lidar around the study tree were locally extracted and RBFs were applied to reconstruct DTMs.

6.2. Post-processing

During post-processing, lidar points were segmented by a semi-automatic method. Two main segmentation methods were used in this study: a marker-controlled segmentation (Chen et al., 2006; Sollie, 2003) and a density and height variance-dependent segmentation. For the purposes of this study, a marker was defined as a treetop location determined from the DCHM. For coniferous trees, the distinguished convex shapes on DCHM were identified easily as treetops. For deciduous trees, however, a tree may contain multiple treetops or a rounded shape. It may, therefore, be difficult to locate tree tops. In these cases, the density and height variance-dependent segmentation method was used. Our process was semi-automatic, because the best segmentation method and parameters used for segmentation were chosen subjectively for each tree case. The main focus of this paper is the wrapped surface reconstruction and does not include the validation of the segmentation method.

6.2.1. A marker-controlled segmentation

All elevation values of lidar points were subtracted by the elevation of DTMs in terms of lidar x and y coordinates. Based on the lidar points without ground elevation, the local maximum lidar points were selected within 1 m × 1 m grid cells to create the DCHM using RBFs. To acquire a smooth and continuous DCHM surface, a 3 × 3 Gaussian filter (Hyyppä et al., 2001) was convolved over the DCHM.

A level set method was used to identify the local peaks of the smooth surface. In this approach, the plane continued progressively through DCHM from bottom to top and 'slices' the DCHM at a certain height. For each sliced plane, a value of 0 is assigned for pixels whose height was less than the height of plane and 1 for all others to create a binary image. For each binary image, a connected component labeling was implemented to label and classify the pixels. To identify the peaks, one sliced image at a certain height was compared with the other sliced image of the next height to see the difference between them. If the total number of labels decreased from one image to the other, the marching sliced plane passed some local peaks of the surface and the locations of the missed local peaks were collected as treetops.

After identifying the local peaks of the surface, we adapted a similar technique which has been used by the marker-controlled segmentation (Chen et al., 2006; Sollie, 2003) and a gradient flow analysis in eight neighboring pixels was used to determine which peak the surrounding pixels belonged to. All pixels were classified based on an identifying number given to each local peak. From the classified image, all discrete lidar points were assigned to point clusters, representing individual trees. Fig. 6 demonstrates the level set method to find a treetop from DCHM.

6.2.2. Density or height variance-dependent segmentation

The marker-controlled method segments lidar points for individual trees based on markers such as tree top location. In the case that a deciduous tree has a rounded shape and one tree top location was not well distinguished, this marker could not be reliably placed and the segmentation did not work well. Since high density lidar data were used and only open canopy trees were used in this study, point density or height variance could be used to segment lidar points. The tree canopy yielded a higher point density or height variation of laser returns than other surfaces, such as the ground or building. The relative difference of point density or height variance was used to segment trees for deciduous trees. By using this approach, the artificial
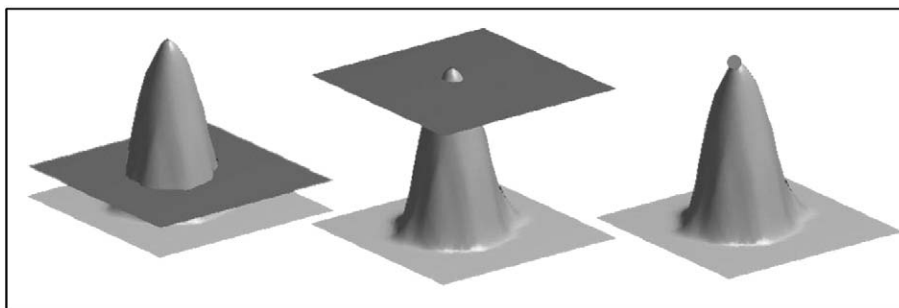

Fig. 6. Level set method is used to identify tree tops. The darker gray plane progresses through the DCHM to identify the peak (treetop, point marker on the right).

objects such as buildings or highway next to the tree were successfully removed. Point density or height variance was calculated in cells, every 1 m × 1 m, based on the lidar points and the threshold value was applied to distinguish between tree crown region and the rest to delineate the crown. However, the edge of the crown could be excluded by the threshold because of a lower point density. A closing morphological image operation (Sollie, 2003) was used on the resulting tree crown delineation map to expand the area by 1 pixel based on the boundary of crown region.

6.2.3. Selecting points for a crown surface

After lidar points representing individual trees without understory vegetation were selected and clustered, their returns came from not only the surface of tree crowns, but also from the interior of the tree crown. For the purpose of surface wrapping, only the points from the surface of tree crowns were required. To remove the points inside the crown, a two-dimensional convex hull algorithm was applied. Lidar points for a single tree were sorted descending according to height. From the maximum height downwards, every 10% of the total number of lidar points was collected, projected in horizontally in two dimensions, and assessed with a two-dimensional convex hull procedure. A three-dimensional convex hull can be applied at once, which results in selecting only outlined points from scattered points and overestimating the shape of tree crown. The piecewise two-dimensional convex hull, therefore, preserves more points represent the complexity of a tree crown.

6.2.4. Wrapping process

After the convex hull process, the selected points were used in the wrapping process. The wrapping was made using Radial Basis Functions (RBFs) and an isosurface algorithm (Angel, 2003) to visualize the implicit surface. The basic idea is to use our lidar data to reconstruct a scalar function $f(x, y, z)$ such that the set of points is calculated as follows;

$$S = \{(x,y,z) : f(x,y,z) = 0\} \tag{1}$$

Eq. (1) is a good approximation to a "wrapping" of the tree crown. We then use an algorithm to construct a triangulation of the surface S. This triangulation can be used for visualization purposes and to estimate crown volume. The isosurface algorithm creates a triangle which uses a subset of voxels. It uses the triangular polygons to tessellate the interpolated intersections and form triangular meshes through voxels (Angel, 2003). Angel (2003) discussed mesh simplification to avoid overestimation of triangular meshes when the intersected triangular polygons pass through the cells. The most common way to simplify the triangular meshes is the well-known Delauney triangulation (Angel, 2003). The mesh optimization was also discussed by Hoppe (1994). In this study, we used an isosurface function built into Matlab (MathWorks Inc., USA).

The isosurface method carries the information pertaining to the nth dimension and projects them into the $(n-1)$th dimension. A good example of this is the contour line. A contour line on a topographical map represents elevation values of three-dimensional topography using two-dimensional line feature. The isosurface method can perform a similar transformation from four dimensions to three dimensions.

Lidar data has three dimensional point locations (X, Y, and Z coordinates). The fourth dimension incorporated into our method is a Euclidean distance. The distance was measured from any arbitrary point or points in space to the closest points on the surface of the tree crown. The distance was analytically measured by RBFs. RBFs produced the distance of all regularly generated points to the closest surface in three dimensions. The isosurface method was then applied to create contour surface of zero distance (Eq. (1)), which was defined as the surface of the tree crown.

6.2.4.1. RBFs and isosurfaces.
Radial Basis Functions (RBFs) constitute one of the exact interpolation methods in three-dimensional space. RBFs in this research were used in two ways: to create DTMs from the classified ground lidar points and to create a wrapping surface from points selected with the convex hull procedure. The general formula of RBFs is given in Eq. (2).

$$f(j) = \sum_{i=1}^{N} \lambda_i \Phi(\|x_i - x_j\|) + \pi(x) \tag{2}$$

where $\pi(x)$ is a polynomial term for point $x \in \Re^3$ $x_i - x_j$ is the Euclidian distance.

λ_i is the weighting coefficient.
N is the number of initial points.
The radial basis function Φ used in this study is $\Phi(r) = r$ (linear).

To generate DTMs, elevation values were given by the function $f(x)$ where x was a two-dimensional vector. We used a fourth dimension to create a wrapping surface for the analytical function $f(x)$ where x was a three-dimensional vector. The wrapped surface was then given by the set of points that satisfies $f(x) = 0$. For this study, the polynomial term of Eq. (2) was null, because it was desired that the resulting interpolated surface should go through all initial points.

To apply RBFs in lidar tree crown research, the coefficient λ_i (the right hand side of Eq. (2)) could be evaluated using the selected points from the convex hull algorithm initially. Since the surface of tree crown represented a distance of zero with respect to the RBFs, all values on the left hand side of the Eq. (2) were zero. With only zero distance, all values of the coefficient λ_i were also zeros. Therefore, two additional sets of points (outside and inside of the desired surface) were required to calculate the coefficient λ_i. The additional points were generated using the normal vector of the selected points. The normal vectors were generated using principal components analysis (Wendland, 2005). Finally, the total $3N$ points were used to solve the linear system. With the given coefficients λ_i using $3N$ points, the distance of any arbitrary points $x \in \Re^3$ in the space is evaluated by the formula below:

$$f(x) = \sum_{i=1}^{3N} \lambda_i \|x_i - x\| \tag{3}$$

where x is any points in $\Re^3$.

Regularly spaced points are generated in two dimensions to create the DTM and in three dimensions to create the wrapped tree crown surface. These points are applied to Eq. (3) to measure the elevation value for DTMs and distance values for the fourth dimension of the wrapping process.

To complete the wrapping process, a routine available in Matlab was used to determine the isosurface of $f(x) = 0$. This routine gave us a triangulation of the surface, which could be used for surface visualization and for the following computation of crown volume.

6.2.4.2. Crown volume estimation using calculus divergence theorem.
Crown volume was calculated from a surface triangulation using the calculus divergence theorem, given by:

$$\text{Volume} = \int_C \nabla F dV = \int_{\partial C} F \overline{n} dS \tag{4}$$

where $F \in \Re^3$ and the surface normal $\overline{n} = (n_x, n_y, n_z)$. By choosing $F = (x, 0, 0)$, we then have $\nabla F = 1$. Therefore,

$$\text{Volume} = \int_{\partial C} F \vec{n} dS = \sum_{j=1}^{m} \overline{n}_j^x \int_{T_j} x dS \tag{5}$$

where: n_j^x is the x-component of the normal to triangle j.

6.3. Validation of tree parameters given by the wrapped surface

To validate the result, a ray-tracing algorithm was used to measure the distance between the closest surface of the wrapped surface and field sampled points using the total station. Established ground GPS locations for fieldwork sometime did not match precisely with lidar point location provided by IMU and GPS during lidar data acquisition. If the field sampled point coordinates tied to the differentiated GPS were slightly shifted from the lidar point distribution for the same tree, this misalignment between them was corrected. Since lidar provides the most reliable and accurate coordinate of tree location, field measured sampled points were repositioned based on lidar-derived stem location as needed.

6.3.1. Ray-tracing algorithm

A ray-tracing algorithm (Glassner, 1989) was applied to calculate the minimum distance between the crown profile points captured by fieldwork and the wrapped surface. Forward ray tracing is defined below:

$$R(t) = R_0 + R_d * t \qquad (6)$$

where R_0 is a initial location of three-dimensional vector, R_d is a three-dimensional vector, and t is a time step. $R(t)$ is the intersected point location at time step t.

The ray/plane intersection algorithm (Glassner, 1989) was used in this study, because the wrapped surface was composed of many
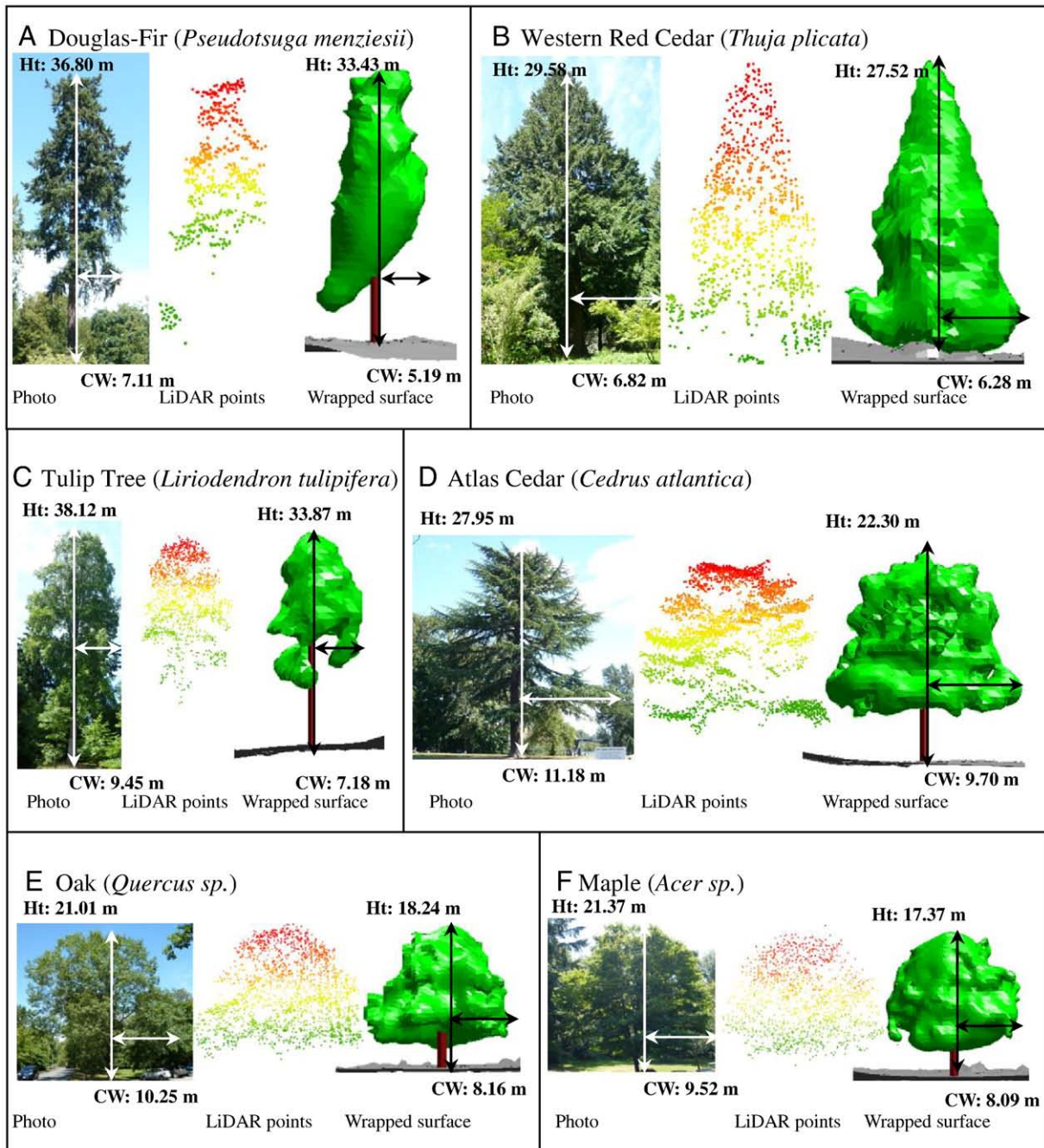

Fig. 7. Visualization of the wrapped surface reconstruction. Shown are Douglas-fir (A), western red cedar (B), tulip-tree (C), atlas cedar (D), oak (E), and maple (F). Ht: Tree Height, CW: Crown width.
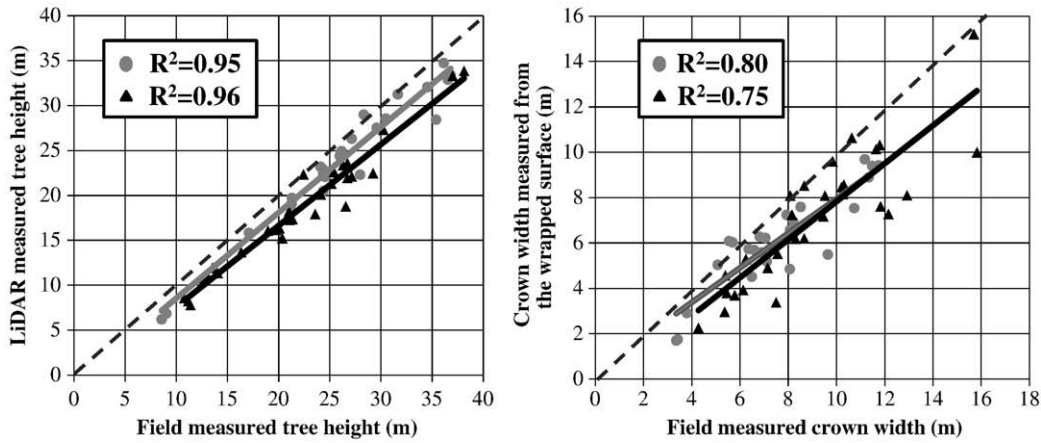
Fig. 8. Correlation of tree height (left) and crown width (right) measurement. Coniferous tree height and crown width are shown by gray circles and line and deciduous tree height and crown width are shown by black triangle and line. The dashed line represents a one-to-one correlation. All *p*-values are 0.00 (*p*<0.05).

triangular polygons. A ray was shot from each field-measured crown profile point (R_0) to the wrapped surface. R_d, the normal vector for each R_0 point, was calculated by principal component analysis (Wendland, 2005). If the ray intersected one of the facets of the wrapped surface, the three dimensional coordinates were recorded as the closest point on the wrapped surface. The distance was measured between the closest point and the sampled point location. That distance was defined as the error between the field-measured point and the wrapped surface. Validation was accomplished in three different ways. In the first, field-measured tree parameters such as tree height, crown width, height of the lowest brunch, and crown base height were compared with tree parameters derived from the wrapped surface. The error of these tree parameters was quantified using the three-dimensional array of the ray-tracing algorithm, since R_d was a three-dimensional vector. In the second, the error variance associated with canopy height was captured using a horizontal two-dimensional ray-tracing algorithm (R_d was a two-dimensional vector) at each height of field sampled points. For the third, the distance between each point used for wrapping process (selected lidar points from convex hull) and the closest point of the wrapped surface was measured using three-dimensional array of ray-tracing algorithm (R_d was a three-dimensional vector). The objective was to prove the exact interpolation of the wrapped surface.

7. Results

7.1. Tree parameters given by the wrapped surface

The wrapped surfaces of six sampled trees are shown in Fig. 7. The wrapped surface goes exactly through the selected points on the tree canopy, as seen in the figure. The complexity of tree canopy was thus captured and visualized by the wrapped surfaces. The error associated with this interpolation was addressed in the Discussion section.

In the following subsection, tree parameters given by the wrapped surface are compared with field measured tree parameters for all 55 sampled trees. Tree height, crown width, crown base height, and crown volume had high correlation between field and the wrapped surface measurement, but the height of the lowest branch had low correlation in the case of the deciduous trees.

7.1.1. Tree height and crown width measurement

The tree height measurement was highly correlated between lidar and field measurements ($R^2 = 0.95$, RMSE = 1.56 m and $R^2 = 0.96$, RMSE = 1.41 m for coniferous and deciduous trees, respectively, Fig. 8). The both *p*-values are significant (*p*<0.05). Lidar-measured tree heights of both the coniferous and deciduous trees were slightly underestimated. The underestimation effect was larger for deciduous trees than for coniferous trees.
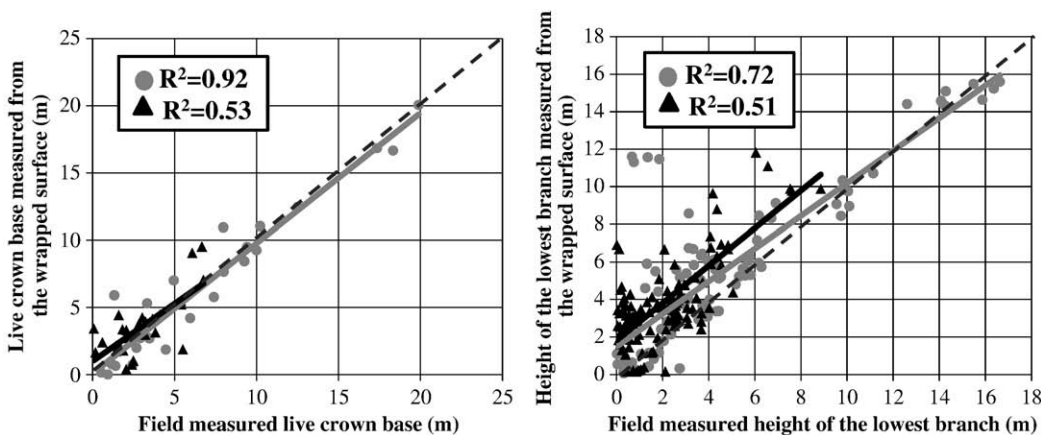

Fig. 9. Correlation of live crown base (left) and height of the lowest branch (right) measurement. Live crown base and height of the lowest branch for coniferous trees are shown by grey circles and line and for deciduous trees are shown by black triangles and line. Dashed line represents one-to-one correlation. All *p*-values are 0.00 (*p*<0.05).
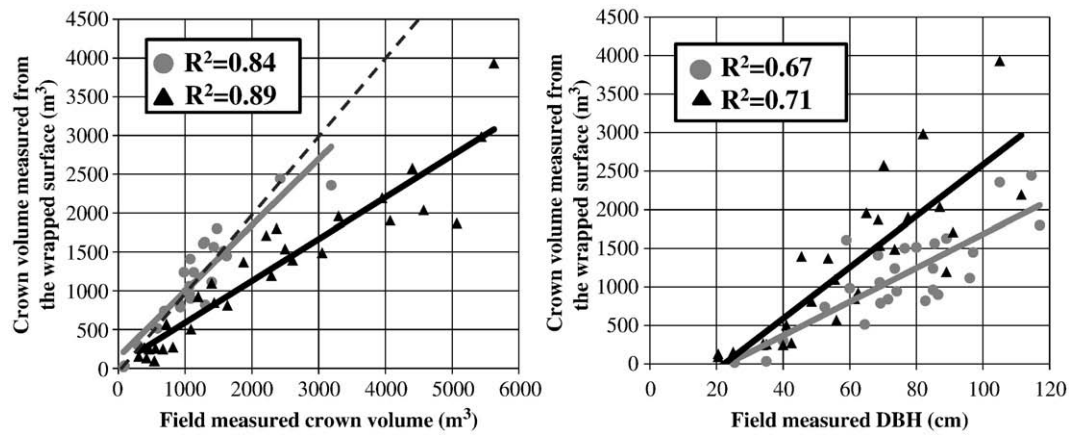
Fig. 10. Correlation of crown volume estimation between field and wrapped surface measurement (left) and crown volume derived from the wrapped surface and field measured DBH (right). Grey circles and line represent coniferous trees and black triangles and line represent deciduous trees. Dashed line represents one-to-one correlation. All *p*-values are 0.00 ($p<0.05$).

The crown width measurement also was highly correlated between lidar and field measurements ($R^2=0.80$, RMSE = 0.93 m and $R^2=0.75$, RMSE = 2.89 m for coniferous and deciduous, respectively, Fig. 8). The crown width measurements of coniferous trees were more strongly correlated than those of deciduous trees. The crown width as estimated by wrapped surface was underestimated for the both coniferous and deciduous trees. The underestimation of the crown width of deciduous trees was larger than that of the coniferous sample.

7.1.2. Crown base height and height of the lowest branch measurement

Crown base height and height of the lowest side branch were compared between field measurement and the wrapped surface measurement. Live crown base and height of the lowest branch for coniferous trees showed a high correlation. Live crown base and height of the lowest branch of coniferous trees had R^2 of 0.92 (RMSE = 1.62 m) and 0.72 (RMSE = 1.54 m) respectively (Fig. 9). Those parameters given by the wrapped surface showed a strong relationship and a one-to-one correlation (within 95% confidential interval of slope). The same tree parameters for deciduous trees had lower correlation and height of the lowest branch for deciduous was more overestimated than that of coniferous trees. Live crown base and height of the lowest branch of deciduous trees showed an R^2 of 0.53 (RMSE = 2.23 m) and 0.51 (RMSE = 1.73 m) respectively (Fig. 9). The lower correlation was found for live crown base and the height of the lowest branch for deciduous trees.

7.1.3. Crown volume measurement

Crown volume estimates from field measurement and the wrapped surface estimate were compared for both coniferous and deciduous trees. Crown volume estimation was highly correlated for both coniferous ($R^2=0.84$, RMSE = 243.31 m^3) and deciduous trees ($R^2=0.89$, RMSE = 328.49 m^3) (Fig. 10). Crown volumes were more likely to be underestimated for deciduous trees than for coniferous trees. Since conventional studies used DBH as an independent variable in crown volume estimation, the relationship of crown volume to field-measured DBH was also assessed. DBH was related to the wrapped surface-generated crown volume for both coniferous ($R^2=0.67$, RMSE = 3.53 m) and deciduous trees ($R^2=0.71$, RMSE = 5.33 m).

Crown volumes were validated with per species field measurements (Fig. 11). The crown volumes of Douglas-fir and western red cedar are shown separately in the figure. For Douglas-fir, there was a lower correlation of this parameter than for western red cedar, but the regression line was in a nearly one-to-one relationship for both species. There was no statistical significance for the case of Douglas-fir, because we have noticed that Douglas-fir trees typically have less regular shapes than western red cedar and more variation of crown volume within

species for Douglas-fir. The variation within species was quantified easily and accurately using the wrapped surface process.

8. Discussion

8.1. Validation of the wrapped surface

8.1.1. The error distance between points and the wrapped surface

There were several basis functions used in previous studies. Carr et al. (1997) used thin-plate spline RBFs for skull reconstruction from 3D CT scan imagery. And Carr et al. (2001) used poly-harmonic spline RBFs for the scattered points of objects scanned by 3D range scanners in situ. In this study, the linear radial basis function was used to get a more exact shape from the existing lidar point cloud and avoided the smoothed and circularly around the surface of tree crowns. To validate this assumption, the distance between selected points using wrapped surface reconstruction and the resulting surface is measured in three dimensions. Table 4 shows the error range of the mean and standard deviation for all sampled trees. The mean range of coniferous trees is between −0.05 and 0.01 m and that of deciduous trees is between 0.04 and 0.5 m. The range of standard deviation for coniferous and deciduous trees is between 0.04 and 0.5 and between 0.03 and 0.65, respectively. The ranges of both mean and standard deviations of distance is larger for deciduous trees than for coniferous trees, because deciduous trees are generally more irregular in shape and the points are thus scattered in a more irregular manner. We may conclude, therefore, that error of this interpolation method does not
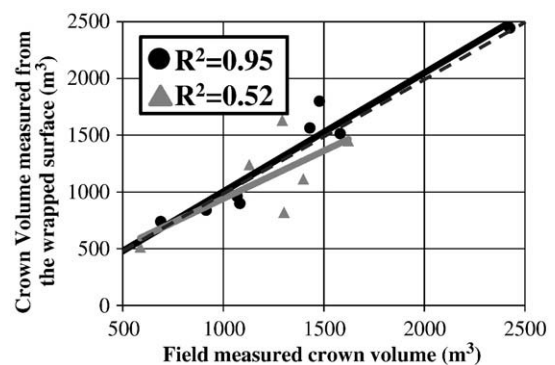

Fig. 11. Crown volume estimation between field and wrapped surface measurement and crown volume derived from the wrapped surface for Douglas-fir (black circles and line) and western red cedar (grey triangles and line). Dashed line represents one-to-one correlation. *p*-value in the case of Douglas-fir is 0.11 ($p>0.05$) and *p*-value in the case of western red cedar is 0.00 ($p<0.05$).

Table 4
The distance between input points used for the wrapping process and the wrapped surface.

	Coniferous trees (26 sample trees)	Deciduous trees (29 sample trees)
Mean error range	−0.05 to 0.01 m	−0.09 to 0.04 m
Standard deviation range	0.04 to 0.5 m	0.03 to 0.65 m

influence the estimation of tree parameters from the wrapped surface. The error distance between the points and the wrapped surface is within 7 cm in both horizontal and vertical dimensions.

8.1.2. The numbers of referenced points for normal vectors

The normal vectors were determined by the neighboring points using principal component analysis. The direction of the normal vector was the key factor in smoothing the surface or generating a more complex surface. As the number of referenced points increased, the resulting surface became smoother. To validate the sufficient number of points, different numbers of referenced points (5 to 50 in increments of 5 points) were used to analyze the influence between the numbers of points and crown volume estimation (Fig. 12).

Four different tree shapes were tested to compare the influence of the number of points on crown volume estimation. Atlas cedar (upper left) had the most complex crown shape due to its propensity for long branch extension and flagging. Western red cedar (upper right) has a conical crown shape, while tulip-tree has a parabolic crown shape (lower left), and maple has a spherical crown shape. As the number of referenced points increased, the complex and conical crown shapes tended to decrease in estimated crown volumes and the parabolic and spherical crown shapes tended to increase. If the number of referenced points increased, normal vectors increasingly pointed in a radial direction from the centroid of the wrapped surface and the represented crown shape became simpler and smoother. A smoother surface means

the wrapped surface loses some degree of the complexity of the original crown architecture. When the shape reached the simplest or smoothest form, estimated crown volumes tended to oscillate and the direction of the normal vector no longer influenced the crown volume. In this study, five referenced points were used to retain the complexity of tree form given by the initial lidar points. Since points were irregularly spaced (scattered from the edge of branches and leaves), the optimal number of referenced points for a given application should be considered based on the point geometry and density.

8.2. Tree parameters given by the wrapped surface

The tree height of deciduous trees experienced greater underestimation than that for coniferous trees (Fig. 8), because lidar data were acquired during early spring (leaf-off) and field measurement was done during summer (foliage present). Even though the leaf-off data was used, the lidar-derived tree height measurement of deciduous trees was highly correlated with field measurements.

The lower correlation of deciduous crown widths with lidar-derived values was reported by Morsdorf et al. (2004) because of the asymmetrical shape of some of these crowns. To capture the asymmetry, we used four vantage points to capture four crown width to achieve R^2 values of 0.80 and 0.75 for coniferous and deciduous trees respectively. Smaller deciduous crowns approached a one-to-one correlation, but the slope of the relationship did not parallel the one-to-one correlation line. This suggests that wrapped-surface crown width estimates performed on smaller deciduous trees were less influenced by bias associated with crown asymmetry.

Wrapped-surface estimates of the live crown base are highly correlated with field measurements for coniferous trees. For coniferous trees, the live crown base approximated the one-to-one correlation line, though the height of the lowest branch was slightly overestimated. This indicated that the lidar returns did not always contact the lowest branches, and the returns were most likely reflected from the area around
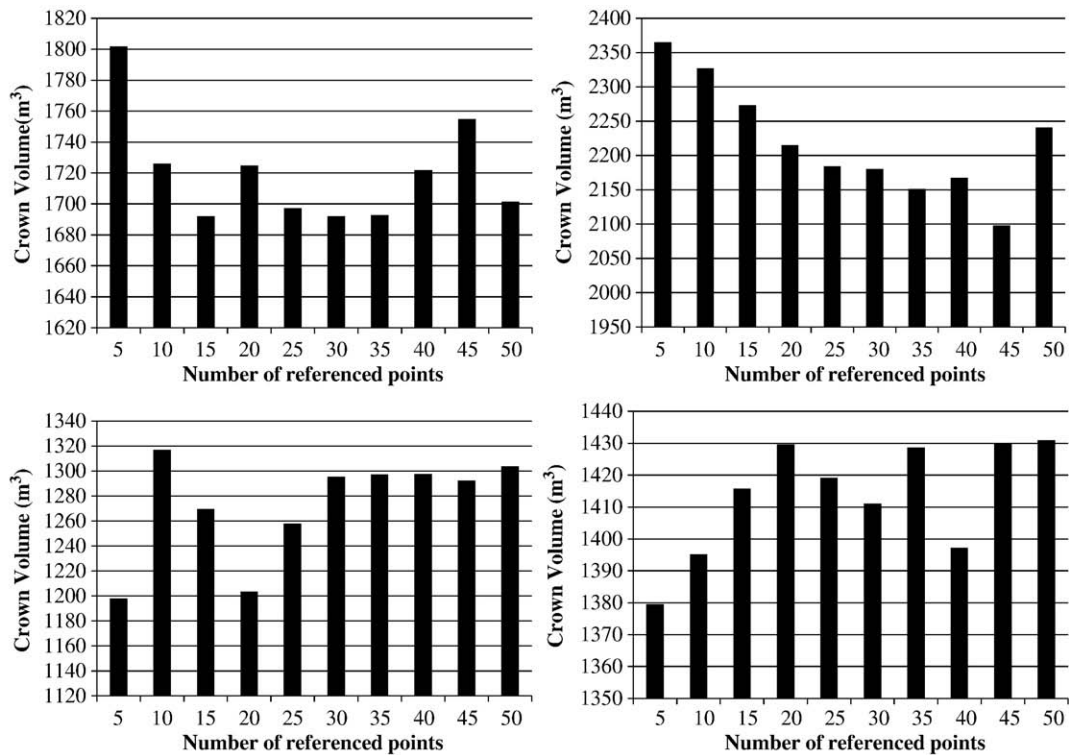

Fig. 12. The influence for crown volume estimation caused by different number of referenced points. Shown are western red cedar (upper left; see also Fig. 7B), Atlas cedar (upper right; Fig. 7D), tulip-tree (lower left; see also Fig. 7C), and maple (lower right; see also Fig. 7E). Note that the y-axis only spans the range of values. To emphasize the effect of crown volume variability, all scales of y-axis are different in this figure.
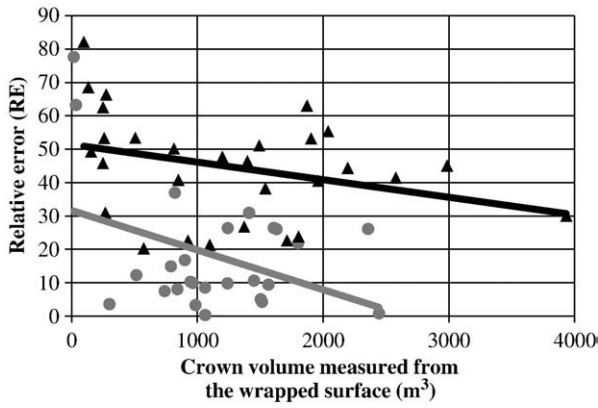
Fig. 13. Crown volume and relative error for coniferous trees (grey circles and line) and deciduous trees (black triangles and line). The line represents the trend of the relationship. As crown volume increases, relative error decreases.

the live crown base for coniferous trees. For deciduous trees, there was more overestimation of the live crown base and the height of the lowest branch. Even though leaf-off data was used to get more returns from lower branches, the tips of the lowest branches was reliably captured by lidar because of attenuation and scatter of the pulses through the canopy. This factor was also partly responsible for underestimation of crown width.

Crown volume estimates derived from the wrapped surface method were highly correlated with field measurements for both coniferous and deciduous trees. The crown volume was slightly overestimated for smaller coniferous trees, but underestimated for larger trees. To assess the effect of tree growth, the relative error of crown volume is shown in Fig. 13. As the crown volume increased, the relative error decreased due to the relatively

smaller proportion of change attributed to crown growth. Two years of growth between lidar acquisition and field measurement may mean a 20% change in height, for example, for small trees, but only a 2% change in height for large trees. Younger trees may be growing more rapidly, and a given height increment is proportionally much greater for a small tree than for an older and larger tree near its maximum height.

Conventional approaches to measuring individual tree crown parameters such as tree height, crown width, and shape to capture crown formation include lidar (Andersen et al., 2002), destructive field sampling (Maguire & Hann, 1989), and interpretation of high resolution imagery (Sheng et al., 2001). Especially, our approach could contribute to calculating tree crown volume precisely and efficiently for an open canopy tree of any species, obviating the need to calculate species-dependent shape parameters to reconstruct the tree crown. Sheng et al. (2001) found that crown shape experiences unique changes as a function of age for different tree species. The wrapped surface method avoids the need to address this complexity, since it can fit any crown shape and overcomes the disadvantages associated with ambiguity of explicit and parametric methods of tree crown reconstruction.

8.3. Error of canopy height

Lefsky et al. (1999) assumed that most reflected energy comes from the local upper canopy surface. To identify how much depth of tree canopy the lasers can detect with high point density lidar data, the horizontal distance between the wrapped surface and field measured points was plotted according to percentile height classes (normalized height by the maximum height for each tree; Fig. 14).

Relatively larger error variance was found at less than 20% height area and between 70% and 90% height area. The error increased toward both the tree top and the bottom of the canopy. The error decreased within the
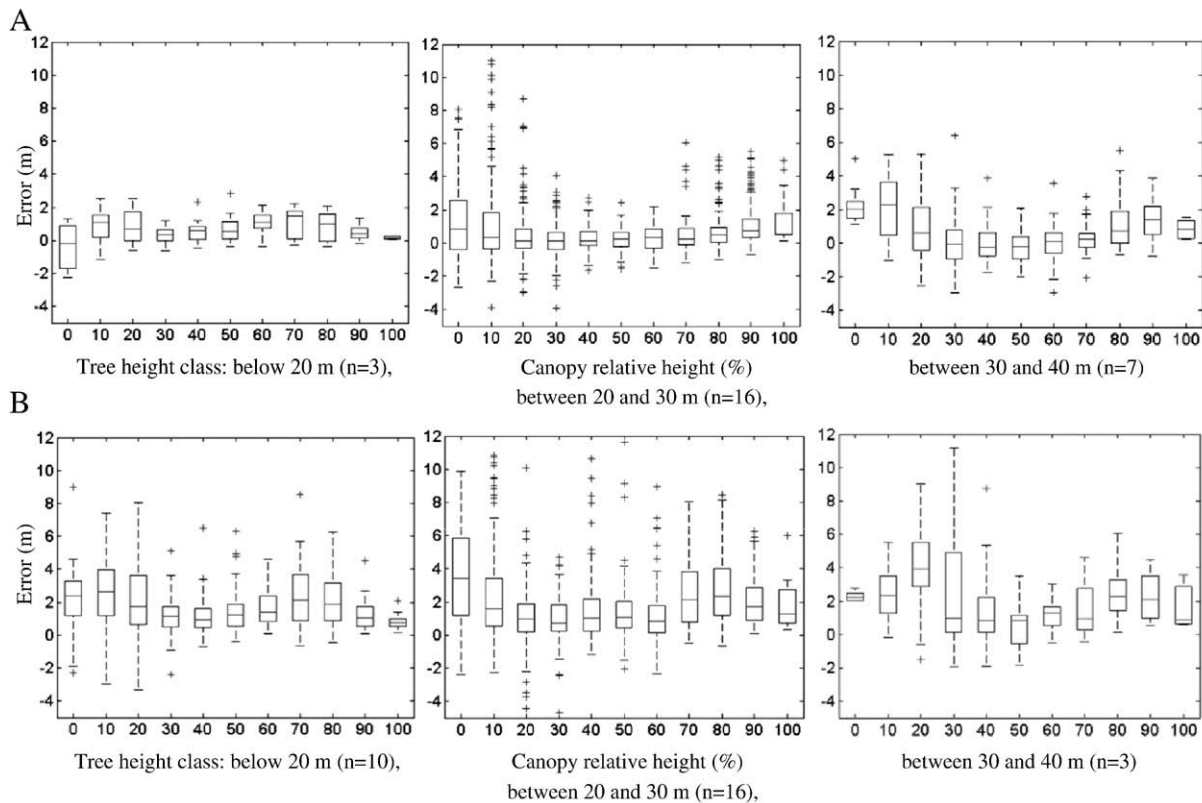

Fig. 14. Box plot of error associated with relative canopy height for coniferous trees (A) and deciduous trees (B) with different height classes. Plus signs are outliers beyond 95% confidential interval.

range of 40% to 60% relative height for both deciduous and coniferous trees. The error around tree tops (70 to 90%) was attributed to the underestimation of lidar measurement for tree tops and error from tree growth over the two-year interval between data acquisition and field measurement. Two years of growth may make a detectable difference at the result from between 20 and 30 m height class coniferous trees that are still growing. Deciduous trees also grow during the two years interval, but the effect of data acquisition during leaf-off season was more important than the effect of tree growth.

The lower region of the canopy (relative height less than 20%) experienced fewer returns due to attenuation of the lidar pulse. The 40% to 60% range was the best predictor of crown formation for any irregular crown shape and for both coniferous and deciduous species. This finding should be considered for change analysis for tree growth using multitemporal lidar data.

8.4. Application of the wrapped surface

The wrapped surface approach described in this paper can be applied to a number of fields including tree physiology, wildland fire management, inventory analysis, and forest management. For example, pipe model theory (Oohata & Shinozaki, 1979; Shinozaki et al., 1964) states that the cross-sectional area of stems and branches at some height was proportional to the total amount of foliage above the height. The crown volume, which is associated with photosynthetic activity, can be quantified by the wrapped surface. When done so, the cross-section of stems can be predicted at any height and stem volume can be estimated easily without destructive sampling. Furthermore, Shinozaki et al. (1964) found that DBH is the best predictor of foliage biomass, and our study found high correlation between DBH and crown volume (Fig. 10), thus, the crown volume derived from the wrapped surface can be a good alternative predictor for foliage biomass (Bortolot & Wynne, 2005) and potentially carbon content (Patenaude et al., 2004) The wrapped surface can also produce more precise dimensions of crown width at any vertical height for the purposes of tree physiological analysis. Point density and space enclosed by the wrapped surface can yield estimates of crown density which is a useful indicator in tree health monitoring (Schomaker et al., 2007; Zarnoch et al., 2004). Tree health monitoring is, therefore, easily achieved by the wrapped surface.

Crown base height and volume measurements from lidar derived from the wrapped surface can improve simulation of fire behavior, including the probability of ground fires progressing to the crown under given conditions. Crown fire simulations depend on accurate estimates of crown volume and the three-dimensional connectivity between crowns. The wrapped surface method can provide those parameters to simulate fire spread at fine spatial scales.

Precise tree parameters given by the wrapped surface can be used for change detection of tree growth. Three-dimensional differences between the wrapped surfaces created by multitemporal aerial or terrestrial lidar data can be used to show the crown growth characteristics for a given tree species. Furthermore, the shape recognition of irregular tree crowns through the wrapped surface method can aid in distinguishing tree species on a morphological basis. Brandtberg (2007) reported that the intensity value of lidar data should be calibrated for use in species identification by using height thresholds to classify the intensity values between ground and canopy. With our method, the angle and direction of tree crown illumination can be distinguished between interior and crown surface lidar points, thus, allowing for the calibration of the intensity value. Furthermore, the structural component derived from the wrapped surface may improve micro-scale shading technique in individual tree level and fusion technique with the other 2D images such as high resolution hyper spectral images for species classification.

Since RBFs were exact interpolators and sensitive to the location of individual points, one important requirement for wrapped surface reconstruction is precise segmentation. We limited our study to open-grown trees for validation of the wrapped surface technique. For managed forest or stands with closed canopies, the segmentation method is critical for precise estimation of tree parameters. Once the points are well segmented, the wrapped surface fits exactly to the segmented points Current segmentation methods do not work well for stands with closed canopies or plantations, however, thinned areas can be used to estimate the tree parameters from the wrapped surface to apply them to predict parameters in the entire area, since lidar point cloud acquired over thinned stands is easily segmented for individual trees. A few sampled trees can be retained in harvest units with sufficient spacing to conduct accurate segmentation of lidar points. These open canopy trees may then be captured by lidar flight to efficiently obtain precise tree parameters. The tree parameters given by the few sampled trees can be applied to estimate the total biomass loss in the harvested area. In this way, it is no longer necessary to measures all crown diameters on fallen trees.

As an alternative way to use this wrapping technique over closed canopy or vertically overlapped trees in the setting of natural forest, entire forest can be wrapped as one enclosed object without segmenting points for individual trees. Though the computation to wrap the huge area is quite expensive, it is possible to estimate an entire area using one wrapped object.

9. Conclusion

A graphic approach named wrapped surface reconstruction using RBFs and isosurfaces was taken to derive tree parameters from lidar discrete points for coniferous and deciduous tree species in an urban forest environment. Our approach was species-invariant, and accurately yielded tree parameters, especially crown volume.

The total station was used to capture entire crown formation accurately from four different cardinal angles, thus minimizing manual errors associated with other devices and avoiding destructive sampling. Accurate georeferencing of all field measured points collected with the total station was critical for comparison with lidar-derived crown reconstructions. As described above, we used differential GPS to perform this task.

Tree parameters such as tree height, crown width, live crown base, the height of the lowest branch, and crown volume derived from the wrapped surface were significantly ($p < 0.05$) correlated with field-measured tree parameters using the total station for both coniferous and deciduous tree species. The lower correlation observed was found for the height of the lowest branch and live crown base for deciduous trees, which was caused by seasonal difference between field observation and lidar acquisition as well as less energy returns from the tips and fine branches at leaf-off lidar data for deciduous trees. To identify errors using the relative height within the canopy, horizontal distance between field observation and wrapped surface was measured. We showed that less than 20% canopy height was always influenced by the effect and 40–60% canopy height was the best predictor of the detection of open canopy tree formation. The error did not come from the RBFs interpolation method itself, because RBFs are one of exact interpolation methods and the exactness was validated in this paper.

Through the capture of micro-scale tree parameters this technique can be useful to many fields such as tree physiology, forest fire, and inventory analysis. Moreover, this technique can be applied to higher point density given by ground-based lidar to capture the micro-scale crown formation analysis. The important requirement of this technique is segmentation method where additional research should be focused. If the points for individual trees are segmented well, tree parameters are automatically derived from the wrapped surface.

Acknowledgement

References

Agee, J. K. (1993). *Fire ecology of Pacific Northwest Forests* (pp. 113–118). Covelo, CA: Island Press.

Andersen, H. E., Reutebuch, S. E., & Schreuder, G. F. (2002). Bayesian object recognition for the analysis of complex forest scenes in airborne laser scanner data. *ISPRS commission III, symposium 2002 Graz, Austria* pages A-035 ff.

Andersen, H. E., Reutenbuch, S. E., & McGaughey, R. J. (2006). A rigorous assessment of tree height measurements obtained using airborne LIDAR and conventional field methods. *Canadian Journal of Remote Sensing, 32*(5), 355–366.

Angel, E. (2003). *Interactive Computer Graphics A Top-Down Approach with OpenGL* (pp. 559–593). NY: Addison Wesley.

Biging, G. S., & Gill, S. J. (1997). Stochastic models for conifer tree crown profiles. *Forest Science, 43*(1), 25–34.

Bishop, C. M. (2005). *Neural networks for pattern recognition* (pp. 164–193). NY: Oxford University Press.

Bloomenthal, J., Bajaj, C., Blinn, J., Cani-Gauscuel, M., Rockwood, A., Wyvill, B., et al. (1997). *Introduction to implicit surface* (pp. 126–165). San Francisco, CA: Morgan Kaufmann Publishers, Inc.

Bortolot, Z., & Wynne, R. (2005). Estimating forest biomass using small footpritn LIDAR data: An individual tree-based approach that incorporates. *ISPRS Journal of Photogrammetery & Remote Sensing, 59*, 342–360.

Brandtberg, T. (2007). Classifying individual tree species under leaf-off and leaf-on conditions using airborne lidar. *ISPRS Journal of Photogrammetery & Remote Sensing, 61*, 325–340.

Carr, J. C., Fright, W. R., & Beatson, R. K. (1997). Surface interpolation with radial basis function for medical imaging. *IEEE Transactions on Medical Imaging, 16*(1), 96–107.

Carr, J. C., Beatson, R. K., Cherrie, J. B., Mitchell, T. J., Fright, W. R., McCallum, B. C., et al. (2001). Reconstruction and representation of 3D objects with radial basis functions. *ACM SIGGRAPH 2001, Los Angeles, CA* (pp. 67–76).

Carr, J. C., Beatson, R. K., McCallum, B. C., Fright, W. R., McLennan, T. J., & Mitchell, T. J. (2003). Smooth surface reconstruction from noisy range data. *ACM GRAPHITE 2003, Melbourne, Australia* (pp. 119–126).

Carson, W. W., Andersen, H. -E., Reutebuch, S. E., & McGaughey, R. J. (2004). LIDAR applications in forestry — an overview. *Proceedings of ASPRS 2004 Annual Conference, Denver, CO, May 2004.*

Chasmer, C., Hopkinson, C., & Treitz, P. (2006). Investing laser pulse penetration through a conifer canopy by integrating airborne and terrestrial lidar. *Canadian Journal of Remote Sensing, 32*(2), 116–125.

Chen, Q., Baldocchi, D., Gong, P., & Maggi, K. (2006). Isolating individual trees in a savanna woodland using small footprint LIDAR data. *Photogrammetric Engineering and Remote Sensing, 72*(8), 923–932.

Clawges, R., Vierling, L., Calhoon, M., & Toomey, M. (2007). Use of a ground-based scanning lidar for estimation of biophysical properties of western larch (*Larix occidentalis*). *International Journal of Remote Sensing, 28*(19), 4331–4344.

Finney, M. A. (1998). *FARSITE: fire area simulator-model development and evaluation.* Ogden, UT: USDA Forest Services RMRS-RP-4.

Glassner, A. S. (1989). *An introduction to ray tracing* (pp. 33–77). NY: Academic Press.

Gobakken, T., & Næsset, E. (2004). Estimation of diameter and basal area distributions in coniferous forest by means of airborne laser scanner data. *Scandinavian Journal of Forest Research, 19*, 529–542.

Gobakken, T., & Næsset, E. (2005). Weibull and percentile models for LIDAR-based estimation of basal area distribution. *Scandinavian Journal of Forest Research, 20*, 490–502.

Henning, J. G., & Radtke, P. J. (2006). Detailed stem measurements of standing trees from ground-based scanning lidar. *Forest Science, 52*(1), 67–80.

Hinsley, S. A., Hill, R. A., Gaveau, D. L. A., & Bellamy, P. E. (2002). Quantifying woodland structure and habitat quality for birds using airborne laser scanning. *Functional Ecology, 16*, 851–857.

Holmgren, J., & Persson, Å. (2004). Identifying species of individual trees using airborne laser scanner. *Remote Sensing of Environment, 90*(4), 415–423.

Hopkinson, C. (2007). The influence of flying altitude, beam divergence, and pulse repetition frequency on laser pulse return intensity and canopy frequency distribution. *Canadian Journal of Remote Sensing, 33*(4), 312–324.

Hoppe, H. (1994). Surface reconstruction from unorganized points. PhD dissertation, University of Washington.

Hyyppä, J., Kelle, O., Lehikoinen, M., & Inkinen, M. (2001). A segmentation-based method to retrieve stem volume estimates from 3-D tree height models produced by laser scanners. *IEEE Transactions on Geoscience and Remote Sensing, 39*(5), 969–975.

Kiser, J., Solmie, D., Kellogg, L., & Wing, M. G. (2005). Efficiencies of traditional and digital measurement technologies for forest operations. *Western Journal of Applied Forestry, 20*(2), 138–143.

Lefsky, M. A., Cohen, W. B., Cohen, Parker, G., & Harding, D. J. (2002). LIDAR remote sensing for ecosystem studies. *BioScience, 52*(1), 19–30.

Lefsky, M. A., Harding, D., Cohen, W. B., Parker, G., & Shugart, H. H. (1999). Surface LIDAR remote sensing of basal area and biomass in deciduous forests of eastern Maryland, USA. *Remote Sensing of Environment, 67*, 83–98.

Lim, K. S., & Treitz, P. M. (2004). Estimation of above ground forest biomass from airborne discrete return laser scanner data using canopy-based quantile estimators. *Scandinavian Journal of Forest Research, 19*, 558–570.

Lowman, M. D., & Rinker, H. B. (2004). *Forest canopies* (pp. 139–331). San Diego, CA: Elsevier Academic Press.

Maguire, D. A., & Hann, D. W. (1989). The relationship between gross crown dimensions and sapwood area at crown base in Douglas-fir. *Canadian Journal of Forest Research, 19*, 557–565.

Maltamo, M., Eerikäinen, K., Pitkänen, J., Hyyppä, J., & Vehmas, M. (2004). Estimation timber volume and stem density based on scanning laser altimetry and expected tree size distribution functions. *Remote Sensing of Environment, 90*, 319–330.

Mean, J. E., Acker, S. A., Harding, D. J., Blair, J. B., Lefsky, M. A., Cohen, W. B., et al. (1999). Use of large-footprint scanning airborne LIDAR to estimate forest stand characteristics in the Western Cascades of Oregon. *Remote Sensing of Environment, 67*, 298–308.

Means, J., AckeRBFsitt, S., Renslow, M., Emerson, L., & Hendrix, C. (2000). Predicting forest stand characteristics with airborne laser scanning LIDAR. *Photogrammetric Engineering and Remote Sensing, 66*(11), 1367–1371.

Morsdorf, F., Meier, E., Koetz, B., Itten, K. I., Dobbertin, M., & Allgower, B. (2004). LIDAR-based geometric reconstruction of boreal type forest stands at single tree level for forest and wildland fire management. *Remote Sensing of Environment, 92*(3), 353–362.

Næsset, E., & Økrand, T. (2002). Estimating tree heights and tree crown properties using airborne scanning laser in a boreal nature reserve. *Remote Sensing of Environment, 79*(1), 105–115.

Nelson, R. (1997). Modeling forest canopy heights: The effects of canopy shape. *Remote Sensing of Environment, 60*(3), 327–334.

Oohata, S., & Shinozaki, K. (1979). A static model of plant form-further analysis of the pipe model theory. *Japanese Journal of Ecology, 29*, 325–335.

Patenaude, G., Hill, R. A., Milne, R., Gaveau, D. L. A., Briggs, B. B. J., & Dawson, T. P. (2004). Quantifying forest above ground carbon content using LIDAR remote sensing. *Remote Sensing of Environment, 93*, 368–380.

Persson, Å., Holmgren, J., & Söderman, U. (2002). Detecting and measuring individual trees using an airborne laser scanner. *Photogrammetric Engineering & Remote Sensing, 68*(9), 925–932.

Phattaralerphong, J., & Sinoquet, H. (2005). A method for 3D reconstruction of tree crown volume from photographs: Assessment with 3D-digitized plants. *Tree Physiology, 25*, 1229–1242.

Popescu, S. C., & Zhao, K. (2007). A voxel-based LIDAR method for estimating crown base height for deciduous and pine trees. *Remote Sensing of Environment, 112*(3), 767–781.

Pouderoux, J. & Gonzato, J-C. (2004). Adaptive hierarchical RBF interpolation for creating smooth digital elevation models. *Proceedings of 12th ACM International Workshop on Geographic Information Systems, ACM-GIS 2004, Washington, DC, USA, November 2004.* (pp. 232–240). ACM New York, NY.

Riaño, D., Chuviec, E., Condis, S., González-Matesanz, J., & Ustin, S. L. (2004). Generation of crown bulk density for *Pinus sylverstris L.* from LIDAR. *Remote Sensing of Environment, 92*, 345–352.

Schomaker, M.E., Zarnoch, S.J., Bechtold, W.A., Latelle, D.J., Burkman, W.G., & Cox, S.M. (2007). Crown-condition classification: A guide to data collection and analysis. General Technical Report SRS-102: USDA Forest Services.

Sheng, Y., Gong, P., & Biging, G. S. (2001). Model-based conifer-crown surface reconstruction from high-resolution aerial images. *Photogrammetric Engineering & Remote Sensing, 67*(8), 957–965.

Shinozaki, K., Yoda, K., Hozumi, K., & Kira, T. (1964). A quantitative analysis of plant from the pipe model theory II. Furthuer evidence of the theory and its application in forest ecology. *Japanese Journal of Ecology, 14*(4), 133–139.

Shirley, P. (2005). *Fundamentals of computer graphics* (pp. 301–346). MA: A K Peters Wellesley.

Smith, S. L., Holland, D. A., & Longley, P. A. (2005). Quantifying interpolation errors in urban airborne laser scanning models. *Gegraphical Analysis, 37*, 200–224.

Sollie, P. (2003). *Morphological image analysis principles and applications* (pp. 105–137). NY: Springer.

Song, B., Chen, J., Desanker, P. V., Reed, D. D., Brandshaw, G. A., & Franklin, J. F. (1997). Modeling canopy structure and heterogeneity across scales: From crowns to canopy. *Forest Ecology and Management, 96*, 217–229.

Thomas, V., Treitz, P., McCaughey, J. H., & Morrison, I. (2006). Mapping stand-level forest biophysical variables for a mixedwood boreal forest using LIDAR: An examination of scanning density. *Canadian Journal of Forest Research, 36*, 34–47.

Wendland, H. (2005). *Scattered Data Approximation* (pp. 1–17). Cambridge, UK: Cambridge Monographs on Applied and Computational Mathematics, Cambridge University Press.

Yu, X., Hyyppä, J., Kaartinen, H., & Maltomo, M. (2004). Automatic detection of harvested trees and determination of forest growth using airborne laser scanning. *Remote Sensing of Environment, 90*, 451–462.

Zarnoch, S. J., Bechtold, W. A., & Stolte, K. W. (2004). Using crown condition variables as indicators of forest health. *Canadian Journal of Forest Research, 34*, 1057–1070.

Zeide, B., & Pfeifer, P. (1991). Fractal dimension is used to characterized tree crown. *Forest Science, 37*(5), 1253–1265.

Zimble, D. A., Evans, D. L., Carlson, G. C., Parker, R. C., Grado, S. C., & Gerard, P. D. (2003). Characterizing vertical forest structure using small-footprint airborne LIDAR. *Remote Sensing of Environment, 87*, 171–182.